Journal of Cellular Biochemistry 101:1329–1337 (2007)

FAST TRACK

PlexinD1 Deficiency Induces Defects in Axial Skeletal Morphogenesis

Tomoatsu Kanda,[1] Yutaka Yoshida,[2] Yayoi Izu,[1] Akira Nifuji,[1] Yoichi Ezura,[1] Kazuhisa Nakashima,[1]* and Masaki Noda[1,3,4]*

[1]Department of Molecular Pharmacology, Medical Research Institute, Tokyo Medical and Dental University, 3-10 Kanda-Surugadai 2-Chome, Chiyoda-ku, Tokyo 101-0062, Japan
[2]Department of Biochemistry and Molecular Biophysics, Howard Hughes Medical Institute, Columbia University, New York, New York 10032
[3]21st Century Center of Excellence (COE) Program for Frontier Research on Molecular Destruction and Reconstruction of Tooth and Bone
[4]Integrated Action Initiative in JSPS Core to Core Program, Japan

Abstract Axial patterning in embryonic skeletogenesis associates with coordinated programming of somitogenesis and angiogenesis. As seen in endochondral bone formation, skeletogenesis is closely related to angiogenesis during development. PlexinD1 is a member of plexin family, is expressed in central nervous system and endothelium, and plays a role in blood vessel patterning and endothelium positioning during embryonic development. Here, we examined the effects of PlexinD1 deficiency on skeletogenesis. Three-dimensional micro CT examination revealed that PlexinD1 deficiency resulted in axial skeletal patterning defects including malformation in vertebral body and rib bone shape. Histological examination of the vertebral bodies and long bones showed that PlexinD1 deficiency altered the development of cartilage. PlexinD1 deficiency did not affect the levels of von Willebrand factor staining in relatively large vessels not attached but close to the vertebral body of mice. However, PlexinD1 deficiency reduced the von Willebrand factor (vWf) staining in most of the microvasculatures attached to the vertebral bone. PlexinD1 was expressed in osteoblastic cells and bone tissues of newborn and adult mice. As most of the homozygous knockout mice did not survive, we examined the role of PlexinD1 in bone formation in heterozygous adult mice subjected to bone marrow ablation. However, PlexinD1 heterozygous knockout did not reveal defects in new bone formation. In conclusion, PlexinD1 is involved in the patterning of axial skeletogenesis. J. Cell. Biochem. 101: 1329–1337, 2007.

Key words: PlexinD1; skeletogenesis; axial patterning; bone formation

Axial skeletogenesis is based on proper somitogenesis along with angiogenesis in the intersomatic regions [Coultas et al., 2005]. After somitogenesis, vertebral bodies are formed through endochondral bone formation [Christ et al., 2004]. Endochondral bone formation occurs in the growth plates at the caudal and rostral ends of vertebral bodies to replace cartilaginous rudiments with bone matrix [Ortega et al., 2004]. This replacement associates with invasion of vessels into the cartilage [Kronenberg, 2003]. Thus, axial bone development and vessel formation are closely related to each other during embryonic development.

During the somitogenesis, PlexinD1 was shown to be involved in somitic vascular patterning [Gitler et al., 2004; Eichmann et al., 2005]. Plexins are trasmembrane molecules, known to play a role in development of immune system as well as axon guidance [Kikutani and Kumanogoh, 2003]. Semaphoring 3E (Sema3E), the ligand of PlexinD1, also controls vascular patterning as well [Gu et al., 2005]. Semaphorins

Grant sponsor: Japanese Ministry of Education; Grant numbers: 18109011, 18659438, 18123456; Grant sponsor: NASDA; Grant sponsor: JSPS.

*Correspondence to: Masaki Noda, Kazuhisa Nakashima, Department of Molecular Pharmacology, Medical Research Institute, Tokyo Medical and Dental University, 3-10 Kanda-Surugadai 2-Chome, Chiyoda-ku, Tokyo 101-0062, Japan. E-mail: noda.mph@mri.tmd.ac.jp

Received 22 January 2007; Accepted 26 January 2007

DOI 10.1002/jcb.21306

act as axon guidance molecules through their cognate plexin receptors [Tamagnone et al., 1999]. Thus, plexins and semaphorins appear to control the vessel pattern formation along with the axial structures through angiogenesis and axon guidance.

Axial skeletogenesis is based on the migration of cells from somites during embryonic development [Olsen et al., 2000]. As semaphoring–plexin interaction plays a role in the determination of axial vascular patterning [Kruger et al., 2005], such actions in vasculogenesis could influence segmental patterning of the skeletogenesis. The aim of this study was to investigate the possible roles of PlexinD1 in skeletogenesis with an interest in the axial bone patterning in embryonic development.

MATERIALS AND METHODS

Animals

PlexinD1 mutant mice (129SVJ and C57BL/6 mixed background) were produced as described previously by Yoshida et al. [Gu et al., 2005]. Heterozygous PlexinD1 mutant mice and control littermates were generated by mating heterozygous PlexinD1 mutant mice. All animal experiments were approved by animal welfare committee of our institute.

Genotyping

PCR genotyping was performed using two sets of primers. PlexinD1 wild type allele was detected by using 5′-ACC GCA GAA CCG GTC ACC GTG TT-3′ (forward primer) and 5′-GGT TAA GGT CGA AGG TGA AGA GCT T-3′ (backward primer). GFP sequence in mutant allele was detected by using 5′-ATG GTG AGC AAG GGC GAG GA-3′ (forward primer) and 5′-TTA CTT GTA CAG CTC GTC CA-3′ (backward primer).

Histological Analysis of Bone

Newborn mice were sacrificed and internal organs were removed. The bodies were fixed in 4% paraformaldehyde (PFA) for 2 h, rinsed with PBS for 30 min, and placed in 30% sucrose in PBS overnight at 4°. For 3D micro CT analysis, these samples were refixed in 70% ethanol at room temperature. After micro CT scanning, embryos were decalcified in EDTA at 4° for 48 h, dehydrated with gradients of ethanol (70, 85, 92.5, and 100%) and xylene and embedded in paraffin. Sections were prepared at 7 μm in thickness and were stained with toluidine blue or hematoxylin and eosin.

Immunohistochemistry

To examine a marker protein of vascular endothelial cells, we performed immunohistochemistry for von Willebrand factor (vWf) using streptavidin-biotin-peroxidase complex (sABC) method. After blocking of endogenous peroxidase, the deparaffinized sections were treated with 0.4 mg/ml proteinase K (Sigma) in 0.01 M phosphate buffered saline (PBS, pH 7.4) for 6 min at room temperature. Then, the sections were treated for 30 min with 10% normal swine serum in 0.01 M PBS and subsequently incubated overnight with polyclonal rabbit anti-human vWf (Dako-cytomation) at a dilution of 1:1,000 at 4°. After washing, sections were incubated with biotinylated swine anti-rabbit IgG (Dako-cytomation) at a dilution of 1:500 for 1 h, followed by sABC reagent. To visualize the immunoreactivity, sections were treated with 0.02% 3,3′-diaminobenzidine tetrahydrochloride (Dojindo Laboratories) and 0.005% H_2O_2 for 5 min. Finally, the sections were counterstained by hematoxylin. Stained sections were dehydrated in a graded ethanol series, cleared in Xylene.

Cell Cultures

Osteoblast-like MC3T3-E1 cells were culturd and maintained in alpha minimum essential medium (alpha-MEM) supplemented with 10% fetal bovine serum (FBS). At subconfluence, MC3T3-E1 cells were harvested and total mRNA was extracted. RNA extraction was conducted according to the acid guanidine isothiocyanate phenol/chloroform method.

Tissue Preparation

For RT-PCR analysis, femora and calvariae of newborn mice, and adult femur, calvaria, marrow tissues, and hearts were collected. Tissues were frozen and total RNAs were extracted. Bone marrow tissues were flushed out from femora to extract total RNA.

Reverse Transcriptase Polymerase Chain Reaction Analysis

Reverse transcription was carried out using 1 μg total RNA. Annealing was conducted at

65° for 10 min using 200 ng oligo (dT) primer, and then the mixture was cooled down on ice. Deoxyribonucleotide triphosphate (dNTPs) mix (10 mM), and Moloney murine leukemia virus-reverse transcriptase (200 U) were mixed in a volume of 20 μl, and this mixture was incubated at 37° for 60 min. Reaction mixture (1 μl) was amplified by PCR using rTaq DNA polymerase. After an initial denaturation at 95° for 2 min in GeneAmp PCR system 9700 (PE Applied Biosystems Foster City, CA), amplification was carried out at 94° for 45 s, at 64° for 45 s, and at 72° for 1 min. The amplification cycle was repeated 30 times. PCR primers for the complementary DNA amplification were designed as follows; PlexinD1 primers were 5′-TCA CTT GGG CTG GGA ACT GAC A-3′ (forward, PlexinD1) and 5′-TCT CTC CAC CGT TCT GTG GGC A-3′ (reverse, PlexinD1), glyceraldehyde-3-phosphate dehydrogenase (GAPDH) primers were 5′-TCC ATG ACA ACT TTG GCA TCG TGG-3′ (forward, GAPDH) and 5′-GTT GCT GTT GAA GTC ACA GGA GA-3′ (reverse, GAPDH). As a negative control, reverse transcription was carried out without these enzymes. The PCR products were electrophoresed on a 1.5% agarose gel and the bands were stained with ethidium bromide. As a control, GAPDH mRNA levels were estimated by RT-PCR at 20 cycles. The cycle number was determined so that the PCR product levels were amplified within a liner range.

Bone Marrow Ablation Procedure

PlexinD1 heterozygous knockout and wild-type male mice (33-week old) were used for these experiments. Bone marrow was ablated in the right femora of each animal as follows. Under avertin anesthesia, a hole was made in the intercondylar regions of the femora by using a 26-G needle. Then, the content of the bone marrow was removed by using dental files followed by insertion of a Kirschner wire upto the proximal ends of the femora. The left femora were used as an internal control.

Three-Dimensional (3D) Micro CT Analysis of Bone

Newborn mice were subjected to micro CT analysis using ScanX-mate-E090 (Comscantechno, Kanagawa, Japan). Analysis was conducted at 40 kVp and 200 mA to obtain the contrast on newborn mice. 3D micro CT scanning was performed for whole body. 3D images were reconstructed using TRI 3D-BON (Ratoc, Shinjyuku, Japan) software.

Two-Dimensional (2D) Micro Computed Tomography (Micro CT) Analysis of Bone

The ablated femora and intact were subjected to 2D micro CT analysis using Musashi (Nittetsu-ELEX, Osaka, Japan). The digital data were reconstructed to obtain CT images. Newly formed trabecular bones volume in the methaphyseal region of femora was quantified using Luzex-F Image analyzing system (NIRECO, Tokyo, Japan) as described previously [Shimizu et al., 1998; Tsuji et al., 2004]. The fractional BV/TV was measured within a rectangular region (0.56 mm × 1.82 mm) with its center at the growth plate.

Statistical Analysis

The results were presented as mean values ± SEM. Statistical significance of the difference was evaluated according to Mann-Whitney's *U*-test or ANOVA. *P*-values <0.05 were considered statistically significant.

RESULTS

PlexinD1 Deficient Mice Revealed Axial Skeletal Malformation

To examine the effects of PlexinD1 deficiency on skeletogenesis, 3D micro CT analysis was conducted using newborn littermate mice. The gross skeletal structure of the PlexinD1 knockout (−/−) mice appeared to be similar to control (+/?) with respect to skull and limbs. However, PlexinD1 deficiency induced splitting of the vertebral bodies (Fig. 1A, B). In lateral views, PlexinD1 deficiency resulted in reduction in the height of vertebral bodies (Fig. 1C, D). Horizontal view of the vertebral bodies indicated that even in some of the vertebral bodies, which did not show clear splitting in anteroposterior views, had partial defects (Fig. 1E, F). To quantify this malformation, we examined the rate of anomaly. The fragmentation rate (the number of fragmented vertebrae divided by the number of total vertebrae) along with the body axis was higher at thoracic and lumber regions than that at sacral regions (Fig. 1G). In addition to vertebral anomaly, rib bones

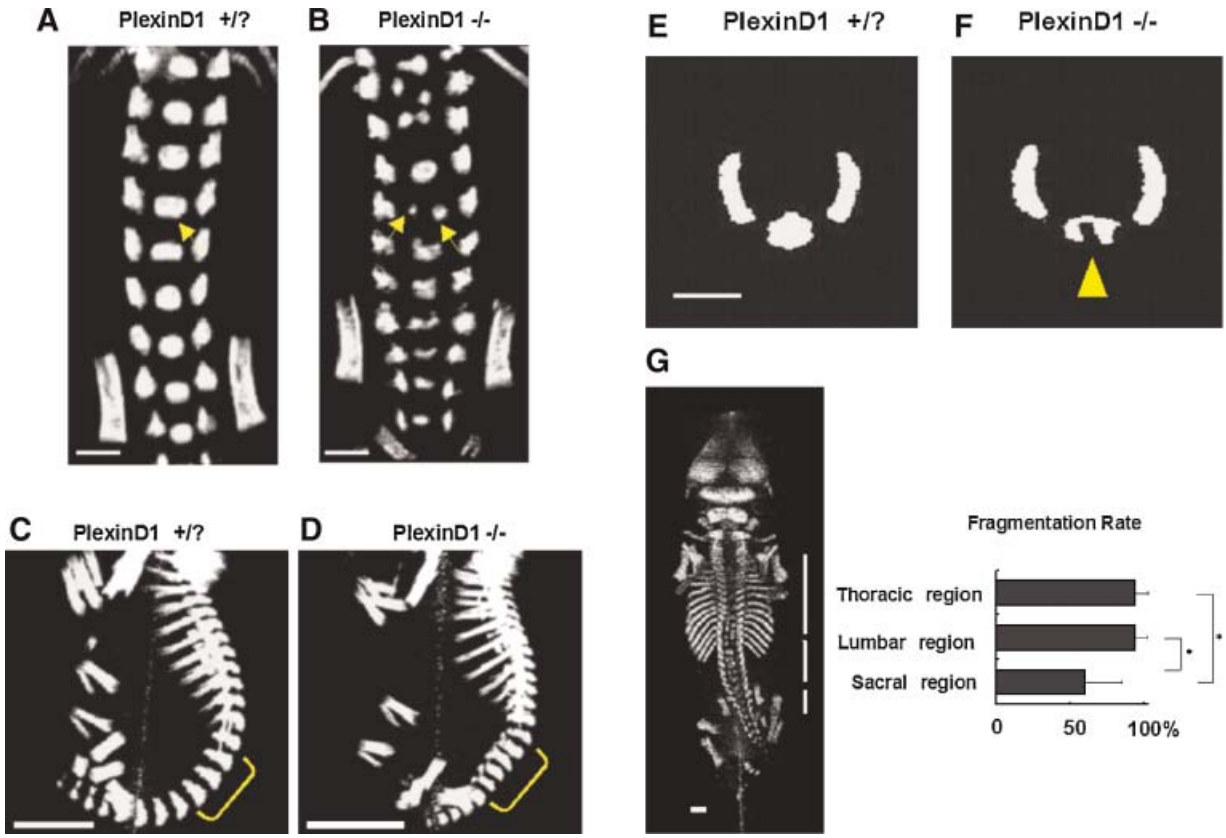

Fig. 1. 3D micro CT analysis on vertebral column. **A**, **B**: Anteroposterior views of the lumber spine. PlexinD1 +/? (A) and PlexinD1 −/− (B) mice. **C**, **D**: Lateral views of the lumber vertebra in PlexinD1 +/? (C) and PlexinD1 −/− (D) mice. **E**, **F**: Horizontal views. (Arrow head indicates defect) Allows indicate splitting of the vertebral body in PlexinD1 −/− (F). **G**: The rate of the vertebral splitting in thoracic, lumber and sacral regions. *, $P < 0.05$. Scale bar (white horizontal line), 1 mm. [Color figure can be viewed in the online issue, which is available at www.interscience.wiley.com.]

exhibited fusions, curving and shortening in PlexinD1 −/− mice (Fig. 2A, B). Regardless of such rib shape anomalies, PlexinD1 −/− mice had normal number of ribs.

Elongation in Hypertrophic Zone of the Growth Plate of PlexinD1 Knockout Mice

To examine the effects of PlexinD1 deficiency on the cells in axial skeletal formation, we examined the histology of bone. In PlexinD1 −/− mice, the number of blood vessel structures close to the vertebral column were not well developed (Fig. 3B) compared to those in control (+/?) mice (closed arrow heads in Fig. 3A). Some of the vertebral body exhibited abnormal cartilaginous protrusion (+/? mice, Fig. 3C; −/− mice, closed arrow head, Fig. 3D). In the growth plates of the long bone, elongation of hypertrophic zone was observed in PlexinD1 −/− mice (Fig. 4B).

Microvasculature Phenotype Associates With Vertebral Body Anomaly in PlexinD1 Knockout Mice

To examine the relationship of the microvasculature development and bone, we performed immunohistochemical studies on vWf, a marker for the endothelial cells in vasculatures. von Willebrand factor was stained intensively in both +/? mice and −/− mice in relatively large vessels which were observed to be close but not attached to the bone surface (Fig. 5A,B, closed arrows). In contrast, PlexinD1 −/− mice still revealed the presence of the microvessels attached to the bone but they were mostly negative in terms of the staining for vWf (Fig. 5D, open arrowheads). Corresponding microvessels in +/? Mice were positive for vWf (Fig. 5E, arrows). In addition, on day 0 postnatally, these vessels were invading into the bone rudiment in wild or heterozygous mice

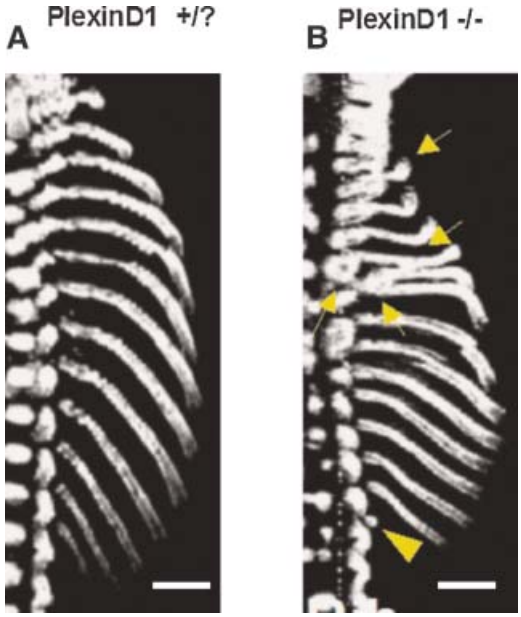

Fig. 2. 3D micro CT analysis on rib malformation. 3D micro CT pictures of the newborn PlexinD1 +/? (**A**) and PlexinD1 −/− (**B**) mice. Arrows indicate curvature as well as fusion of the ribs. Arrow head shows shortening of the rib bone. Scale bars, 1 mm. [Color figure can be viewed in the online issue, which is available at www.interscience.wiley.com.]

(Fig. 5E, arrows indicate blood vessels present in capillary positive for vWf). In contrast, in PlexinD1 −/− mice, such invasion into the bone rudiment, was reduced (Fig. 5F). These features including the reduced levels of vWf-positive vessels which are attaching to the bone and the reduction in the invading vessels into the bone rudiment were compatible with the micro CT observations that vertebral body formation was impaired in PlexinD1 −/− mice.

Osteoblasts Express PlexinD1 mRNA

To see the expression of PlexinD1 in skeletal cells, we examined the levels of mRNA based on RT-PCR analysis using total RNA extracted from bone tissues (Fig. 6). Plexin D1 mRNA was expressed in femora and calvaria of newborn mice (Fig. 6, lanes 5, 6). As these bone tissues contain vessels where PlexinD1 was previously detected, we examined whether PlexinD1 is expressed in osteoblastic cell line. The data revealed that PlexinD1 was expressed in osteoblastic MC3T3-E1 cells (Fig. 6, lane 4). The band size was similar to the control band obtained from heart mRNA (Fig. 6, lane 3). PlexinD1 mRNA was also expressed in adult calvaria, bone marrow and femora (Fig. 6, lanes 7, 8, 9).

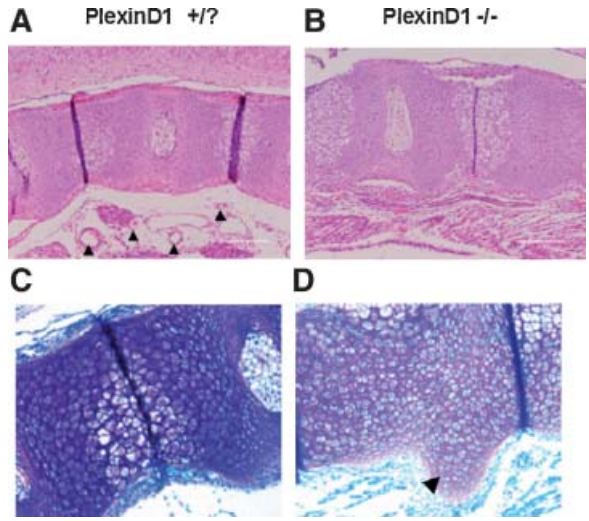

Fig. 3. Histological examination of newborn knockout mice. Histology of the vertebral bone in newborn mice. **A**: Newborn mice indicate vascular structures along with the vertebral column in control mice (dorsal up, rostral right). **B**: Such vascular structures were not clearly observed in PlexinD1 −/− mice. Hypertrophic cartilage morphology was observed in the end plate region of vertebral bone in PlexinD1 +/? Mice (**C**). Hypertrophic cartilage in the vertebral disc zones was not clearly observed in PlexinD1 −/− mice (**D**). Some of the vertebrae indicated protrusion of the cartilaginous tissue from vertebral body (arrow head). A, B: Sagittal sections stained with hematoxylin and eosin. C, D: Toluidine blue staining. Scale bars, 200 μm.

The Levels of Newly Formed Bone were Similar Between Wild-Type and Heterozygous Knockout Mice After Bone Marrow Ablation

As we observed that PlexinD1 is expressed in adult bone and bone marrow tissues as well as in osteoblastic cells, we examined the effect of PlexinD1 on new bone formation in adult mice. For this, we conducted bone marrow ablation experiments. Because PlexinD1 knockout mice

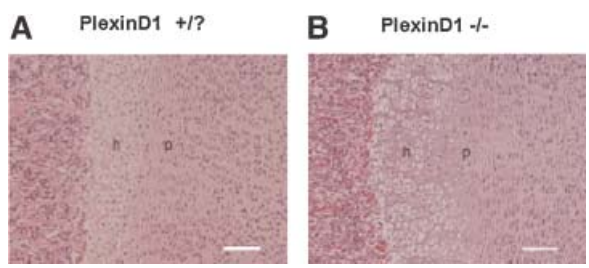

Fig. 4. Growth plate of long bone in newborn mice. Humeri of new born mice were decalcified and sections were stained with hematoxylin and eosin. **A**: Control (+/?) mice. **B**: LexinD1 −/− mice. h, hypertrophic zone; p, proliferating zone. Scale bars, 100 μm. [Color figure can be viewed in the online issue, which is available at www.interscience.wiley.com.]

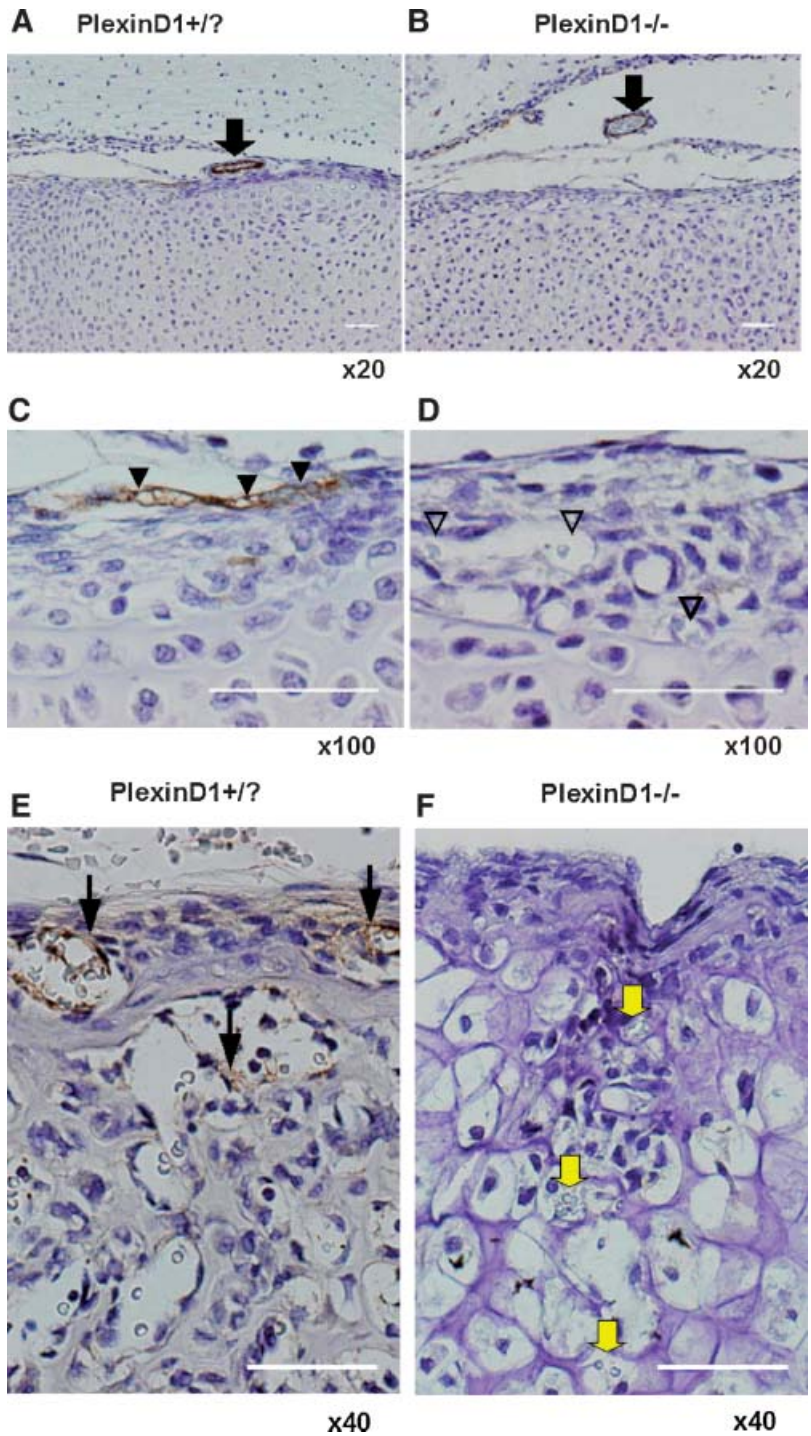

Fig. 5. Distribution of blood vessels in vertebral bodies. Immunohistochemistry was performed with antibody against vWf (**A**–**F**). vWf immunoreactivity was detected in blood vessels of vertebral bodies. vWf immunoreactivity was observed in the large blood vessels, which localized close to the bone surface but were not attached to the bone surface, in both PlexinD1 +/? and −/− mice (A and B, closed arrows). Within the periosteum, the microvasculature was distributed in both PlexinD1 +/? and −/− mice (C, D). In PlexinD1 +/? mice, the microvasculature, including blood cells and having flattened endothelial cells, was vWf immunopositive (C, closed arrowheads). On the contrary, in PlexinD1 −/− mice, vWf immunopositive microvasculature was reduced significantly (D, open arrowheads). (E, F) Magnification of the periosteum attached to the hypertrophic chondrocyte at the thoracic vertebrae (ventral up, rostral left). In PlexinD1 +/? mice, vWf immunoreactivity was observed in vascula around the periosteum and bone rudiment (E, arrows). However, in PlexinD1 −/− mice, no immunoreactivity was observed, although there were a few microvasculature with blood cells in bone rudiment (F, yellow arrows). Scale bars (A–F), 50 μm.

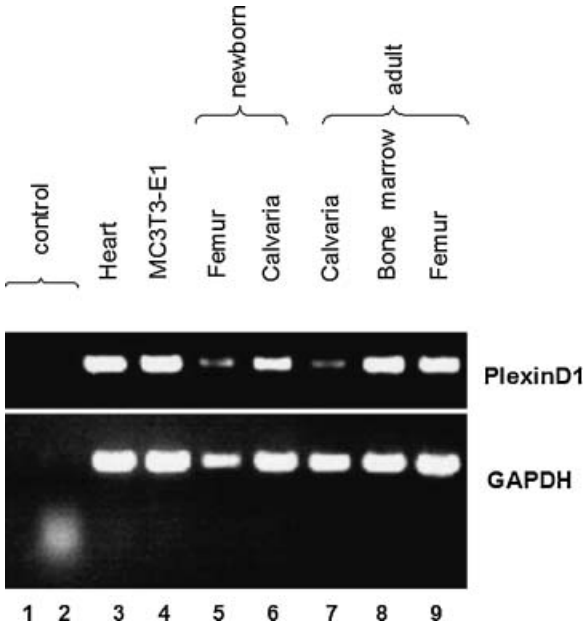

Fig. 6. PlexinD1 mRNA is expressed in bone and osteoblasts. Reverse transcriptase polymerase chain reaction (RT-PCR) was conducted as described in Materials and Methods. Heart tissue was used as positive control (**lane 3**). PlexinD1 expression was detected with MC3T3-E1 cells (**lane 4**). PlexinD1 mRNA was also detected in bone tissues of newborn mice (**lane 5**, femur; **lane 6**, calvaria), and adult bone tissues (**lane 7**, calvaria; **lane 8**, bone marrow, **lane 9**, femur without bone marrow). **Lane 1** (water) and **lane 2** (total RNA 1 μg) as negative controls.

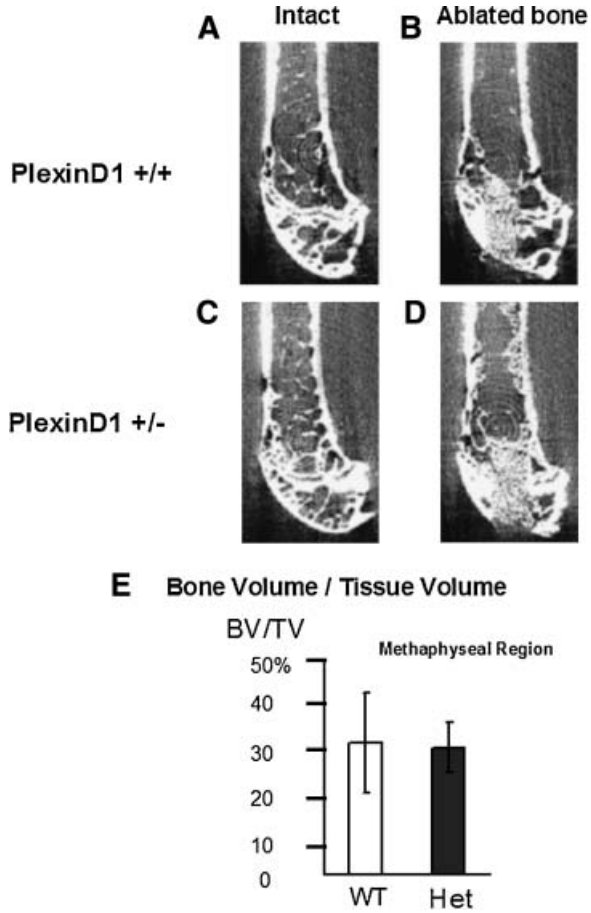

Fig. 7. The levels of newly formed bone after bone marrow ablation were similar in PlexinD1 heterozygous knockout and wild type mice. Wild-type mice (**A**, intact left femur; **B**, ablated right femur) and PlexinD1 heterozygous knockout mice (**C**, intact left femur; **D**, ablated right femur). **E**: Quantification of newly formed bone after bone marrow ablation.

did not survive to adult stage, we used wild-type and heterozygous knockout mice. At ten days after bone marrow ablation, we measured the BV/TV of newly formed bone in the ablated area. The levels of newly formed bone were similar between heterozygous knockout and wild type (Fig. 7A–E).

DISCUSSION

In this study, we reported that PlexinD1 deficiency induced splitting in the vertebral bodies and irregularity in their contour. Furthermore, rib bone patterning was also altered in PlexinD1 knockout mice. Thus, PlexinD1 deficiency affects morphology of axial skeletons. The axial skeletal elements in mice consist of 7 cervical, 13 thoracic, 6 lumber, and 4 sacral vertebrae [Wellik and Capecchi, 2003]. The number of these components was similar between control and knockout mice. The levels of bone mineral density (BMD) were also similar in newborn mice (data not shown). Thus, effects of PlexinD1 deficiency would be mainly observed in terms of the patterning of the axial skeletal elements. These observations imply that PlexinD1 may control the axial skeletogenesis as a molecule required for fine tuning of the formation of vertebral bodies and ribs.

von Willebrand factor staining in PlexinD1 −/− mice was significantly reduced in the microvessels attached to the vertebral bone. Furthermore, microvessel invasion into the bone rudiments as also impaired in PlexinD1 −/− mice. These features were corresponding to the observations on the malformation of the vertebral bodies. Interestingly, larger vessels, which were close to but not attached to the vertebral bone, were positive for vWf in both PlexinD1 +/? and PlexinD1 −/− mice. Thus, PlexinD1 deficiency affects more in the bone-attached vessels than the ones close to but not

attached to bones. These observations suggest close relationship of the bone anomaly to the vascular phenotype.

It was reported that semaphorin β/collapsin1 mutant mice showed rib fusion and partial duplication in ribs [Behar et al., 1996]. Furthermore, Sema3a null mice indicate vascular defects [Serini et al., 2003]. In the case of PlexinD1 knockout mice, we did not observe duplication but fusions between rib bones. Semaphorin 3E (Sema3E), which is a ligand of PlexinD1, is expressed in mesenchymal tissues including the caudal sclerotome and perinotochordal mesenchyme [Miyazaki et al., 1999a,b], and the expression patterns of Sema3E and PlexinD1 are complementary [Gu et al., 2005]. Therefore, the skeletal phenotype in PlexinD1 −/− mice shares, at least with respect to rib malformation, defects with those in Semaphorin −/− mice suggesting that the anomaly may be in part due to the disruption of this ligand-receptor signaling. Although we have shown that osteobalsts (MC3T3-E1) express PlexinD1, whether such signaling defects affect bone patterning indirectly via vessel malformation or directly via skeletogenesis or both is still to be determined.

We observed the abnormality in the thickness of hypertrophic zone in the long bone and in the chondrocyte patterning in the vertebral body rudiments. Invasions of microvessels into hypertrophic cartilages was also reduced in PlexinD1 −/− mice. These observations suggest that PlexinD1 deficiency would influence not only patterning in axial skeleton but also histological features in skeletal tissues. Although PlexinD1 deficiency altered intersomitic vessel patterning, chondrocyte hypertrophy appears to exist. Therefore, we cannot exclude the possibility that PlexinD1 may affect both vessel side and chondrocyte side to lead to these phenotypes.

Recently, it was reported that PlexinA1 mutant mice revealed severe osteopetrosis [Takegahara et al., 2006; Tamagnone and Giordano, 2006], revealing that plexins would act in osteoclastic cell. In the case of PlexinD1 deficient mice, we did not observe any phenotypes related to functional defects in osteoclasts such as osteopetrosis as the null mice did not survive up to the adult stage. Although PlexinD1 is expressed in adult bone, bone marrow ablation experiments did not reveal phenotypes suggesting presences of compensatory system in these heterozygotes or it may be that only null mice could exhibit phenotype. In conclusion, this study revealed that PlexinD1, an axon guidance molecule, plays a role in the development of axial skeletogenesis.

ACKNOWLEDGMENTS

This research was supported by the grants-in-aid received from the Japanese Ministry of Education (21st Century Center of Excellence (COE) Program, Frontier Research for Molecular Destruction and Reconstitution of Tooth and Bone, 18109011, 18659438, 18123456), Grants from Japan Space forum, NASDA, and Japan Society for Promotion of Science (JSPS Core to Core Program on Advanced Bone and Joint Science (ABJS), Research for the Future Program, Genome Science).

REFERENCES

Behar O, Golden JA, Mashimo H, Schoen FJ, Fishman MC. 1996. Semaphorin III is needed for normal patterning and growth of nerves, bones and heart. Nature 383:525–528.

Christ B, Huang R, Scaal M. 2004. Formation and differentiation of the avian sclerotome. Anat Embryol (Berl) 208:333–350.

Coultas L, Chawengsaksophak K, Rossant J. 2005. Endothelial cells and VEGF in vascular development. Nature 438:937–945.

Eichmann A, Le Noble F, Autiero M, Carmeliet P. 2005. Guidance of vascular and neural network formation. Curr Opin Neurobiol 15:108–115.

Gitler AD, Lu MM, Epstein JA. 2004. PlexinD1 and semaphorin signaling are required in endothelial cells for cardiovascular development. Dev Cell 7:107–116.

Gu C, Yoshida Y, Livet J, Reimert DV, Mann F, Merte J, Henderson CE, Jessell TM, Kolodkin AL, Ginty DD. 2005. Semaphorin 3E and plexin-D1 control vascular pattern independently of neuropilins. Science 307:265–268.

Kikutani H, Kumanogoh A. 2003. Semaphorins in interactions between T cells and antigen-presenting cells. Nat Rev Immunol 3:159–167.

Kronenberg HM. 2003. Developmental regulation of the growth plate. Nature 423:332–336.

Kruger RP, Aurandt J, Guan KL. 2005. Semaphorins command cells to move. Nat Rev Mol Cell Biol 6:789–800.

Miyazaki N, Furuyama T, Amasaki M, Sugimoto H, Sakai T, Takeda N, Kubo T, Inagaki S. 1999. Mouse semaphorin H inhibits neurite outgrowth from sensory neurons. Neurosci Res 33:269–274.

Miyazaki N, Furuyama T, Takeda N, Inoue T, Kubo T, Inagaki S. 1999a. Expression of mouse semaphorin H mRNA in the inner ear of mouse fetuses. Neurosci Lett 261:127–129.

Olsen BR, Reginato AM, Wang W. 2000. Bone development. Annu Rev Cell Dev Biol 16:191–220.

Ortega N, Behonick DJ, Werb Z. 2004. Matrix remodeling during endochondral ossification. Trends Cell Biol 14: 86–93.

Serini G, Valdembri D, Zanivan S, Morterra G, Burkhardt C, Caccavari F, Zammataro L, Primo L, Tamagnone L, Logan M, Tessier-Lavigne M, Taniguchi M, Puschel AW, Bussolino F. 2003. Class 3 semaphorins control vascular morphogenesis by inhibiting integrin function. Nature 424:391–397.

Shimizu T, Mehdi R, Yoshimura Y, Yoshikawa H, Nomura S, Miyazono K, Takaoka K. 1998. Sequential expression of bone morphogenetic protein, tumor necrosis factor, and their receptors in bone-forming reaction after mouse femoral marrow ablation. Bone 23:127–133.

Takegahara N, Takamatsu H, Toyofuku T, Tsujimura T, Okuno T, Yukawa K, Mizui M, Yamamoto M, Prasad DV, Suzuki K, Ishii M, Terai K, Moriya M, Nakatsuji Y, Sakoda S, Sato S, Akira S, Takeda K, Inui M, Takai T, Ikawa M, Okabe M, Kumanogoh A, Kikutani H. 2006. Plexin-A1 and its interaction with DAP12 in immune responses and bone homeostasis. Nat Cell Biol 8:615–622.

Tamagnone L, Artigiani S, Chen H, He Z, Ming GI, Song H, Chedotal A, Winberg ML, Goodman CS, Poo M, Tessier-Lavigne M, Comoglio PM. 1999. Plexins are a large family of receptors for transmembrane, secreted, and GPI-anchored semaphorins in vertebrates. Cell 99:71–80.

Tamagnone L, Giordano S. 2006. Semaphorin pathways orchestrate osteogenesis. Nat Cell Biol 8:545–547.

Tsuji K, Komori T, Noda M. 2004. Aged mice require full transcription factor, Runx2/Cbfa1, gene dosage for cancellous bone regeneration after bone marrow ablation. J Bone Miner 19:1481–1489.

Wellik DM, Capecchi MR. 2003. Hox10 and Hox11 genes are required to globally pattern the mammalian skeleton. Science 301:363–367.